IL-18 and VEGF-A trigger type 2 innate lymphoid cell accumulation and pro-tumoral function in chronic myeloid leukemia

Benedetta Fiordi,[1,2] Valentina Salvestrini,[3] Gabriele Gugliotta,[3] Fausto Castagnetti,[3] Antonio Curti,[3] Daniel E. Speiser,[4] Emanuela Marcenaro,[5,6] Camilla Jandus[1,2#] and Sara Trabanelli[1,2#]

[1]Department of Pathology and Immunology, Faculty of Medicine, University of Geneva, Geneva, Switzerland; [2]Ludwig Institute for Cancer Research, Lausanne Branch, Lausanne, Switzerland; [3]IRCCS Azienda Ospedaliero-Universitaria di Bologna, Institute of Hematology «Seràgnoli», Bologna, Italy; [4]Department of Oncology, Lausanne University Hospital (CHUV) and University of Lausanne, Epalinges, Switzerland; [5]Department of Experimental Medicine (DIMES), University of Genova, Genova, Italy and [6]IRCCS Ospedale Policlinico San Martino, Genova, Italy

[#]CJ and ST contributed equally as senior authors.

Correspondence: S. Trabanelli
sara.trabanelli@unige.ch

Received: September 20, 2022.
Accepted: March 29, 2023.
Early view: April 6, 2023.

https://doi.org/10.3324/haematol.2022.282140

IL-18 and VEGF-A trigger type 2 Innate Lymphoid Cell accumulation and pro-tumoral function in Chronic Myeloid Leukemia

Short title: ILCs in CML

Benedetta Fiordi,[1,2] Valentina Salvestrini,[3] Gabriele Gugliotta,[3] Fausto Castagnetti,[3] Antonio Curti,[3] Daniel E. Speiser,[4] Emanuela Marcenaro,[5,6] Camilla Jandus[1,2]* and Sara Trabanelli[1,2]*

[1]Department of Pathology and Immunology, Faculty of Medicine, University of Geneva, Geneva, Switzerland.
[2]Ludwig Institute for Cancer Research, Lausanne Branch, Lausanne, Switzerland.
[3]IRCCS Azienda Ospedaliero-Universitaria di Bologna, Institute of Hematology « Seràgnoli », Bologna, Italy.
[4]Department of Oncology, Lausanne University Hospital (CHUV) and University of Lausanne, Epalinges, Switzerland.
[5]Department of Experimental Medicine (DIMES), University of Genova, Genova, Italy.
[6]IRCCS Ospedale Policlinico San Martino, Genova, Italy.

*Equally contributed to the work

Corresponding author: Sara Trabanelli, sara.trabanelli@unige.ch

Supplementary Methods

Flow cytometry analysis

Lineage markers: FITC-conjugated anti-CD3 (REA613, Miltenyi), anti-CD4 (REA623, Miltenyi), anti-CD8 (REA734, Miltenyi), anti-CD14 (REA599, Miltenyi), anti-CD15 (VIMC6, Miltenyi), anti-CD19 (REA675, Miltenyi), anti-CD20 (REA780, Miltenyi), anti-CD33 (REA775, Miltenyi), anti-CD34 (AC136, Miltenyi), anti-CD203c (NP4D6, Biologend) and anti-FcεRI (AER-37 (CRA1), Biologend); Brilliant Violet 421-conjugated anti-CD127 (A019D5, Biolegend), BUV737 conjugated anti-CD56 (NCAM16.2, BD Biosciences), Brilliant Violet 785 anti-CD94 (HP-3D9, BD Biosciences), BUV395-conjugated anti-CRTH2 (BM16, Biolegend) and Brilliant Violet 605-conjugated anti-cKit (104D2, Biolegend). Additional markers: PerCP/Cy5.5-conjugated anti-CD309 (7D4-6, Biolegend), PE-conjugated anti-CXCR7 (10D1-J16, Biolegend), PE/CY7-conjugated anti-CD218a (H44, Biolegend), BV510-conjugated anti-CXCR4 (12G5, Biolegend) and BV711-conjugated anti-NKp30 (P30-15, Biolegend). Samples were acquired on a LSRFortessa (BD). Data were analyzed using FlowJo software (TreeStar V.10).

Cell culture

The human CML cell line K562 was cultured in RPMI 1640 GlutaMAX medium supplemented with 10% FCS (Gibco), 5% penicillin/streptomycin (Thermo-Fisher), 5% HEPES (Thermo-Fisher), 0.05 mM 2β-mercaptoethanol (Thermo-Fisher). Medium was replaced every 2–3 days. Where indicated, human recombinant IL-18 (50 ng/ml, R&D System), IL-13 (50 ng/ml, Peprotech) and CXCL12 (150ng/ml, Peprotech) were added.

Quantitative real-time PCR (qPCR)

Total RNA was isolated using the TRIZOL reagent according to the manufacturer's instructions (Invitrogen). Final preparation of RNA was considered DNA- and protein-free if the ratio of readings at 260/280 nm was ≥1.7. Isolated mRNA was reverse-transcribed by iScript Reverse Transcription Supermix for RT-qPCR (Bio-Rad). The quantitative real-time PCR was carried out in the Applied Biosystems 7900HT Fast Real-Time PCR Sequence Detection System (Applied Biosystems) with specific primers (*AREG*: FW 5'-GAGCCGACTATGACTACTCAGA-3', RV 5'-TCACTTTCCGTCTTGTTTTGGG-3'; NKp30 (*NCR3*): FW 5'- CCCCTGAGATTCGTACCCTG-3', RV 5'-

CTCCACTCTGCACACGTAGAT-3'; *IL13RA1*: FW 5'-TGAGTGTCTCTGTTGAAAACCTC-3', RV 5'- GGGGTACTTCTATTGAACGACGA-3'; *IL13RA2*: FW 5'- GGGCATTGAAGCGAAGATACA-3', RV 5'-GCCCAGGAACTTTGAACTTCTG-3'; *IL5RA*: FW 5'-ATCATCGTGGCGCATGTATTAC-3', RV 5'- AAAGAACTTGAGCCAAACCAGT-3'; *IL4R*: FW 5'-CGTGGTCAGTGCGGATAACTA-3', RV 5'-TGGTGTGAACTGTCAGGTTTC-3'; *EGFR*: FW 5'-TTGCCGCAAAGTGTGTAACG-3', RV 5'-TCACCCCTAAATGCCACC-3'; *VEGFA:* FW 5'-AGG GCA GAA TCA TCA CGA AGT-3', RV 5'-AGG GTC TCG ATT GGA TGG CA-3') using KAPA SYBR® FAST qPCR Kits (Roche). Samples were amplified simultaneously in duplicate in one-assay run with a non-template control blank for each primer pair to control for contamination or for primer dimerization, and the Ct value for each experimental group was determined. The housekeeping gene (beta-2-microglobulin (*β2M*): FW 5'-GAGGCTATCCAGCGTACTCCA-3', RV 5'-CGGCAGGCATACTCATCTTTT-3') was used as an internal control to normalize the Ct values, using the $2^{-\Delta Ct}$ formula.

ELISA

Amphiregulin and prostaglandin D2 concentrations were evaluated using ELISA kits according to the manufacturer's instructions (RayBio).

Cell proliferation assay

ILC2 proliferation ability was tested after 5 days in culture with and without human recombinant IL-18 (50 ng/ml, R&D System) using 1µM CellTrace Far Red staining according to the manufacturer's instruction (Invitrogen). Samples were acquired on a LSRFortessa (BD). Data were analyzed using proliferation analysis on FlowJo software (TreeStar V.10).

Multiplex cytokine assay

The concentrations of various cytokines in cell-free culture supernatants, healthy donors' and patients' sera were determined using multi-LEGENDplex™ analyte flow assay kits (human Th Panel (12-plex), human Neuroinflammation Panel (13-plex), human CXCL12 Panel (1-plex) and Custom human Th Panel (5-plex), Biolegend). The assays were performed according to manufacturer's instructions. Samples were acquired on an Attune NxT Flow Cytometer (Thermo Fisher). Data were analyzed using FlowJo software (TreeStar V.10).

The results were analyzed using the Qognit software by Legendplex.

In vitro co-culture experiments

Healthy donor expanded ILC2s were cultured in StemSpan SFEM II (Stemcell) medium supplemented with 20U/ml human recombinant IL-2 and co-cultured with the K562 CML cell line in a 1:1 ratio or with K562 CM collected after 48h incubation at 10^4 cells/ml. Anti-VEGFR2 (SU1498, Selleckchem) was used at 10µM for 48h and masking NKp30 antibody was added at 5µg/ml (F252) for 30min at 37°C, then washed before co-culture. After 48h, supernatants were harvested and analyzed to detect cytokine production by Legendplex analysis and cell pellets were stored in TRIZOL for qPCR analysis. Where indicated, Dasatinib, Imatinib and Nilotinib (Sigma-Aldrich) were resuspended in DMSO and used at the concentration and time reported.

Chemotaxis assay

In a tranwell system, we added 600µl in the lower compartement either of medium alone or medium with CXCL12 (150 ng/ml) and we seeded 25.000 ILC2s in 100µl in the upper compartment. After 1h, we recovered the bottom medium and measured the ILC2 counts with CountBright Absolute Counting Beads (Thermo Fisher). Samples were acquired on a LSRFortessa (BD) and 5000 beads per each sample were acquired. Data were analyzed using FlowJo software (TreeStar V.10).

Sorting strategy

$CD34^+$ cells were sorted from CML or HD PBMCs. Markers: FITC-conjugated anti-CD4 (REA623, Miltenyi), anti-CD8 (REA734, Miltenyi), anti-CD15 (VIMC6, Miltenyi), anti-CD19 (REA675, Miltenyi), anti-CD20 (REA780, Miltenyi), anti-CD33 (REA775, Miltenyi), anti-CD203c (NP4D6, Biologend); BV711-conjugated anti-CD3 (OKT3, Biologend), anti-CD16 (3G8, Biologend) and anti-CD19 (HIB19, Biolegend); PeCy7-conjugated anti-CD2 (RPA-2.10, Biologend), anti-CD56 (HCD56, Biologend) and anti-CD235a (HIR2, Biologend); BV421-conjugated anti-CD24 (ML5, Biolegend); BUV737-conjugated anti-CD14 (M5E2, Biolegend); PE-conjugated anti-CD34 (561, Biolegend); PE-Dazzle-conjugated anti-CD127 (A7R34, Biolegend) and viability dye DRAQ7 (Invitrogen). After gating for lymphocytes, singlets and alive cells, $CD34^+$ cells were identified as $CD3^-CD16^-CD19^-CD14^-CD24^-CD56^-CD34^+$ and

$CD14^+$ cells were identified as $CD3^-CD16^-CD19^-CD34^-CD14^+$. The sorting was made with BDAria (BD).

Supplementary Table

PATIENT	AGE	SEX	SOKAL*	ELTS**	SPLENOMEGALY	TRANSCRIPT	THERAPY	APPLICATION
1	43	M	LOW	LOW	NO	B2A2/B3A2	IMATINIB	SOLUBLE FACTORS
2	41	M	LOW	LOW	NO	B2A2	NILOTINIB	SOLUBLE FACTORS PHENOTYPE
3	49	F	LOW	LOW	NO	B2A2/B3A2	DASATINIB	SOLUBLE FACTORS PHENOTYPE
4	72	M	INT	INT	NO	B2A2	DASATINIB	SOLUBLE FACTORS PHENOTYPE
5	56	F	LOW	LOW	NO	B2A2	IMATINIB	SOLUBLE FACTORS PHENOTYPE
6	52	F	INT	INT	YES	B2A2/B3A2	NILOTINIB	SOLUBLE FACTORS PHENOTYPE
7	51	F	LOW	LOW	NO	B2A2/B3A2	NILOTINIB	SOLUBLE FACTORS
8	47	F	LOW	LOW	NO	B2A2	NILOTINIB	SOLUBLE FACTORS
9	76	M	INT	INT	NO	B2A2	DASATINIB	SOLUBLE FACTORS
10	63	F	INT	LOW	NO	B2A2	DASATINIB	SOLUBLE FACTORS
11	80	M	INT	INT	NO	B2A2/B3A2	IMATINIB	SOLUBLE FACTORS
12	47	F	LOW	LOW	NO	B2A2/B3A2	NILOTINIB	SOLUBLE FACTORS
13	57	F	INT	INT	NO	B2A2/B3A2	DASATINIB	SOLUBLE FACTORS
14	59	M	INT	LOW	NO	B2A2/B3A2	DASATINIB	SOLUBLE FACTORS
15	54	M	LOW	LOW	NO	B2A2/B3A2	NILOTINIB	SOLUBLE FACTORS
16	54	M	HIGH	HIGH	YES	B2A2	NILOTINIB	SOLUBLE FACTORS
17	61	M	HIGH	HIGH	YES	B2A2	PONATINIB	SOLUBLE FACTORS PHENOTYPE
18	45	M	INT	INT	YES	B3A2	NILOTINIB	SOLUBLE FACTORS
19	83	M	INT	INT	NO	B2A2	DASATINIB	SOLUBLE FACTORS PHENOTYPE
20	73	M	INT	INT	NO	B2A2	DASATINIB	SOLUBLE FACTORS
21	61	F	LOW	LOW	NO	B2A2/B3A2	NILOTINIB	SOLUBLE FACTORS PHENOTYPE
22	37	M	HIGH	HIGH	YES	B2A2	NILOTINIB	PHENOTYPE
23	52	F	LOW	LOW	NO	B2A2	IMATINIB	PHENOTYPE
24	46	M	LOW	LOW	NO	B3A2	NILOTINIB	PHENOTYPE
25	32	M	LOW	LOW	NO	B2A2	IMATINIB	PHENOTYPE
26	38	M	HIGH	HIGH	YES	B3A2	DASATINIB	PHENOTYPE
27	40	F	INT	LOW	YES	B2A2	NILOTINIB	PHENOTYPE
28	25	M	HIGH	HIGH	YES	B3A2	NILOTINIB	PHENOTYPE
29	82	M	HIGH	HIGH	YES	B3A2	IMATINIB	PHENOTYPE
30	70	F	INT	LOW	NO	B2A2	NILOTINIB	PHENOTYPE
31	87	M	HIGH	n.d.	n.d	B3A2	n.d.	PHENOTYPE
32	77	M	INT	LOW	NO	B3A2	NILOTINIB	PHENOTYPE
33	79	F	INT	HIGH	NO	B2A2	IMATINIB	PHENOTYPE

**SOKAL **ELTS (EUTOS Long-Term Survival): risk assessment scoring systems*

Table S1. Clinical data and biological characteristics of the patients included in the study.

n.d. = not determined.

Supplementary Data

Figure S1

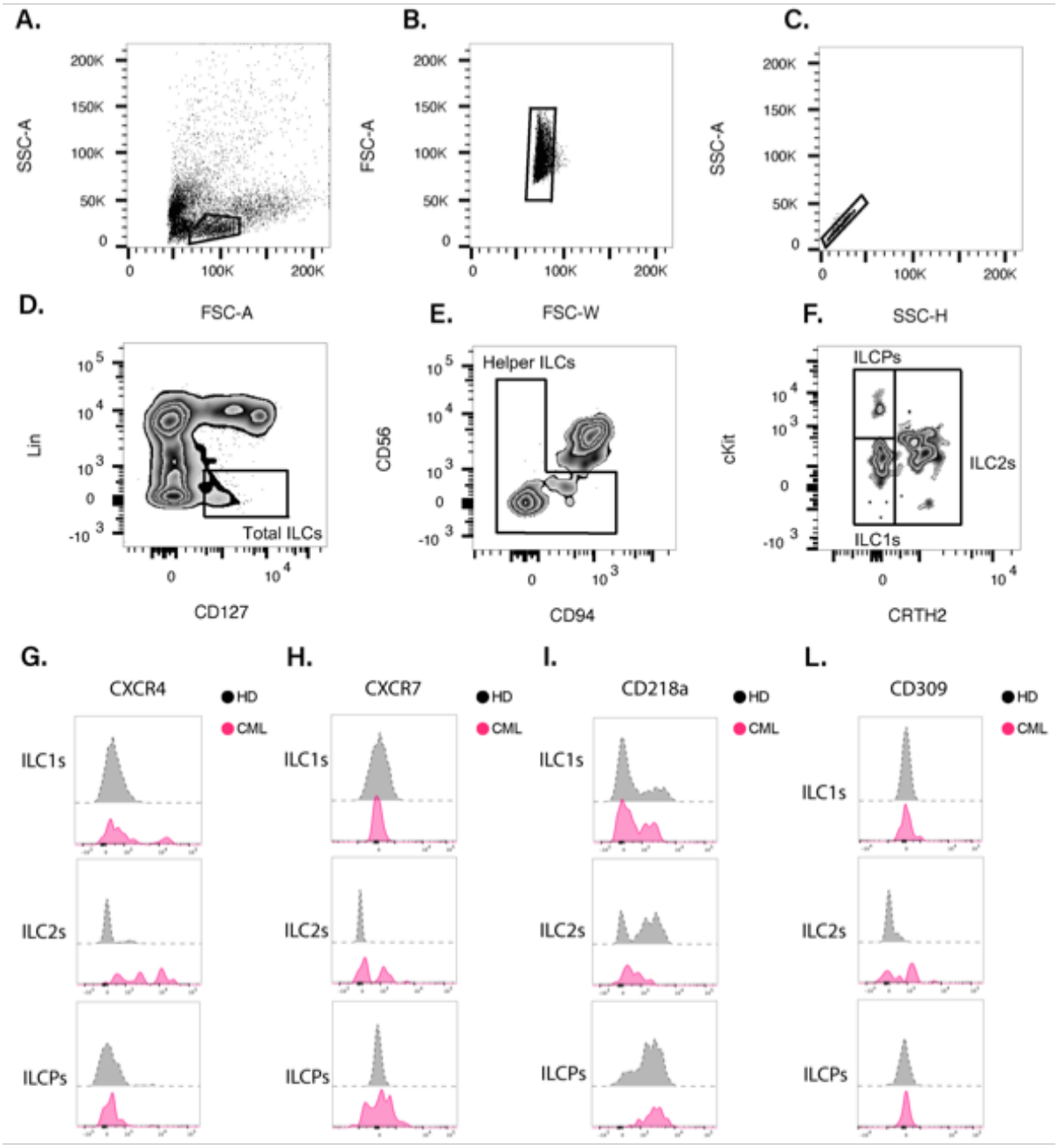

Figure S1. ILC gating strategy in Peripheral Blood Mononuclear Cells (PBMCs) and receptors' expression on the ILC subsets. (A-D) After gating on lymphocytes and singlets,

total circulating ILCs were identified as living Lin^- $CD127^+$ lymphocytes. **(E)** CD56 and CD94 expression was used to define helper ILCs. **(F)** ILC subsets were identified using CRTH2 and cKit expression and defined as: $cKit^-CRTH2^-$ ILC1s; $cKit^{-/+}CRTH2^+$ ILC2s; $cKit^+CRTH2^-$ ILCPs. **(G-H)** Representative histograms of CXCR4 and CXCR7 receptor expression on ILC1s, ILC2s and ILCPs in HD and CML patients. **(I-L)** Representative histograms of IL-18Rα (CD218a) and VEGF-A (CD309) receptors on ILC1s, ILC2s and ILCPs in HD and CML patients.

Figure S2

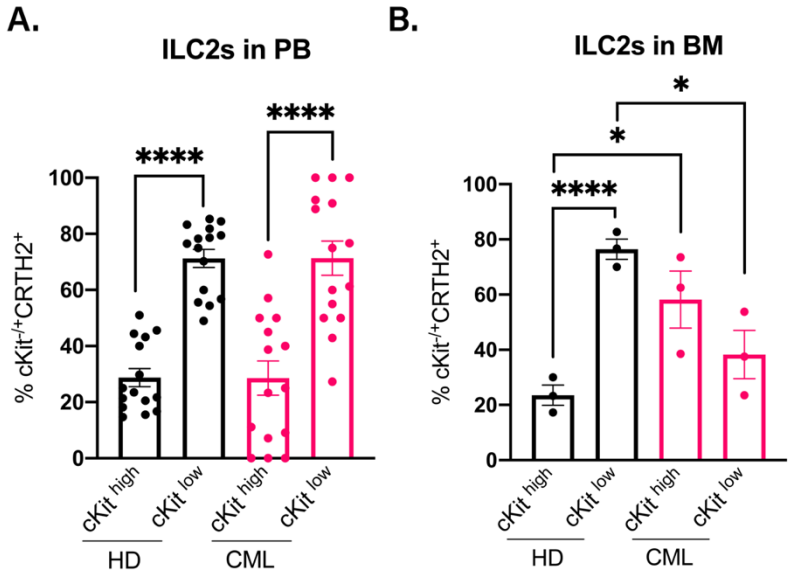

Figure S2. ILC2 cKit^{high} and ILC2 cKit^{low} distribution in the PB and BM of HD and CML patients. (A) ILC2 cKit^{high} and cKit^{low} in the PB of both HD (n=15) and CML patients (n=21) **(B)** ILC2 cKit^{high} and cKit^{low} (n=3 for both cohorts). Statistical analysis: Mann-Whitney test and unpaired t test, *p=<0.05; **p=<0.01; ***p=<0.001; ****p=<0.0001.

Figure S3

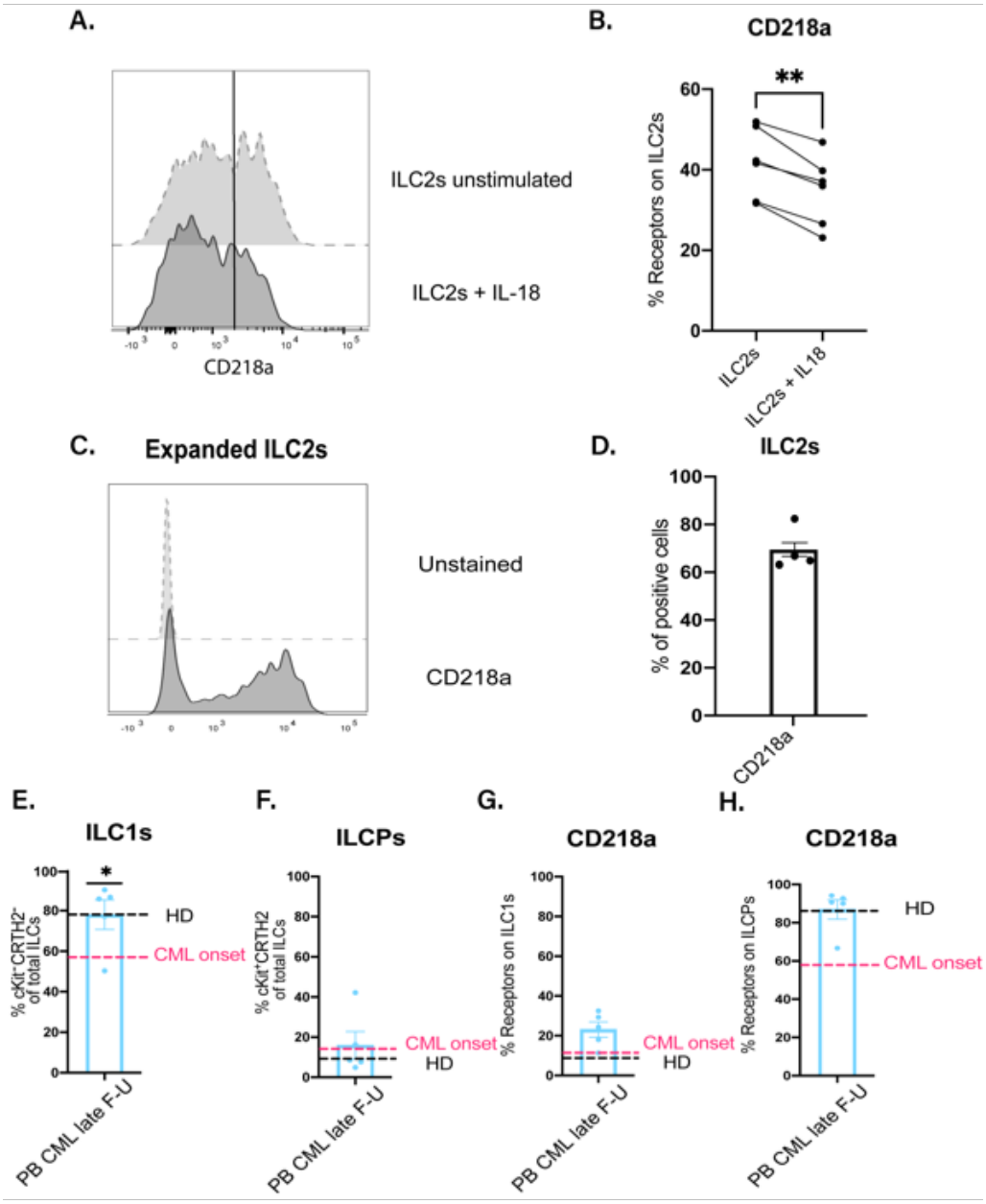

Figure S3. CD218a is downregulated on ILC2s after stimulation with IL-18 and ILC1s are restored after TKIs treatment. (A) CD218a expression in control and stimulated ILC2s. **(B)** Quantification of CD218a expression on ILC2s upon IL-18 stimulation for 48h (n=6). **(C-D)** Expression of IL-18 receptor (CD218a) on expanded ILC2s from HD (n=4). **(E-F)** ILC1s and ILCPs in CML PB at late (>12 months) (n=5) follow-ups (F-U). **(G-H)** CD218a expression

on ILC1s and ILCPs in CML PB at late (>12 months) (n=5) follow-ups (F-U). Statistical analysis: two-way ANOVA, *p=<0.05; **p=<0.01; ***p=<0.001; ****p=<0.0001.

Figure S4

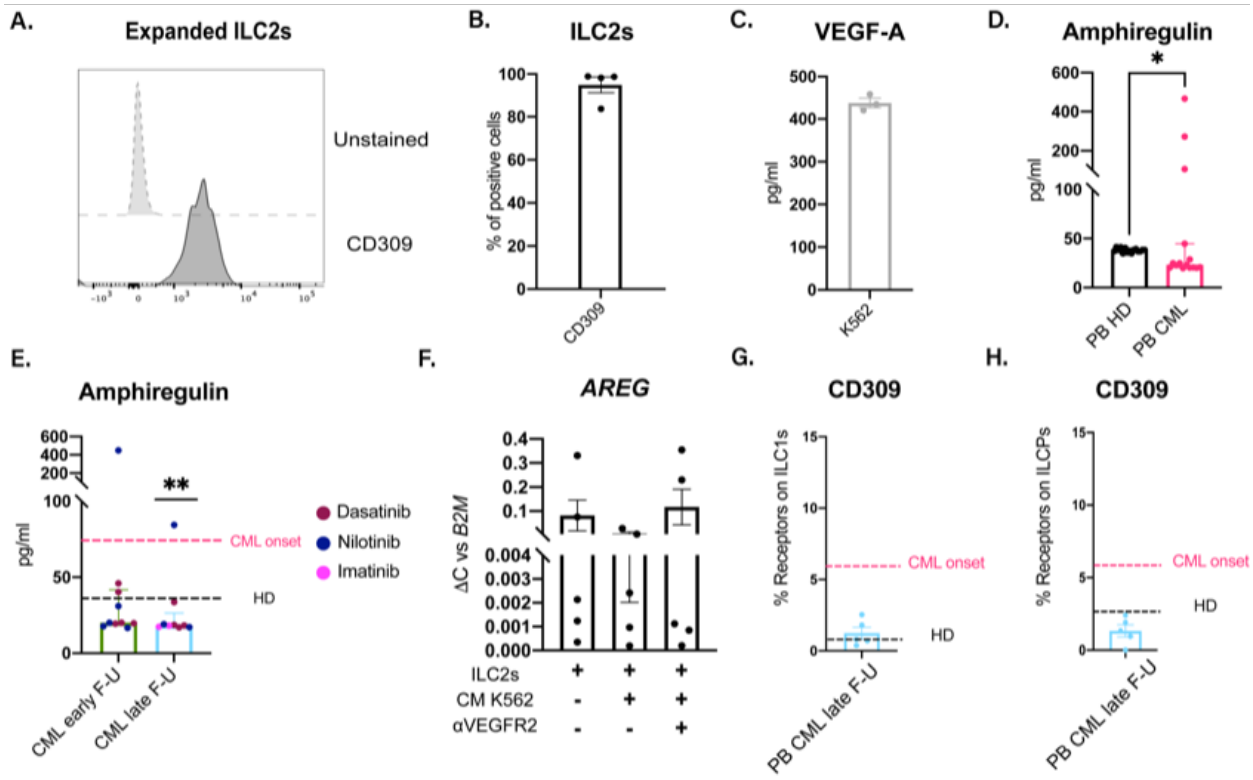

Figure S4. AREG gene expression is not significantly affected in K562 and ILC2 co-culture but it is decreased after TKIs treatment in patients. (A-B) Expression of VEGF-A receptor (CD309) on expanded ILC2s from HD (n=4). **(C)** VEGF-A secretion (pg/ml) by K562 cell line at 48h. **(D)** Amphiregulin (AREG) concentrations (pg/ml) in CML patients' sera at diagnosis (n=21) versus HD (n=15). **(E)** AREG levels in CML sera after different treatments at early (<12 months) (n=15) or late (>12 months) (n=11) follow-ups (F-U). **(F)** AREG gene expression normalized on B2M in ILC2s stimulated with the CM of K562 in the presence or not of the VEGFR2 inhibitor (10µM, SU-1498) (n=5). **(G-H)** CD309 expression on ILC1s, ILC2s and ILCPs in CML PB at late (>12 months) (n=5) follow-ups (F-U). Statistical analysis: Mann-Whitney test, paired and unpaired t test, ordinary one-way ANOVA and two-way ANOVA, *p=<0.05; **p=<0.01; ***p=<0.001; ****p=<0.0001.

Figure S5

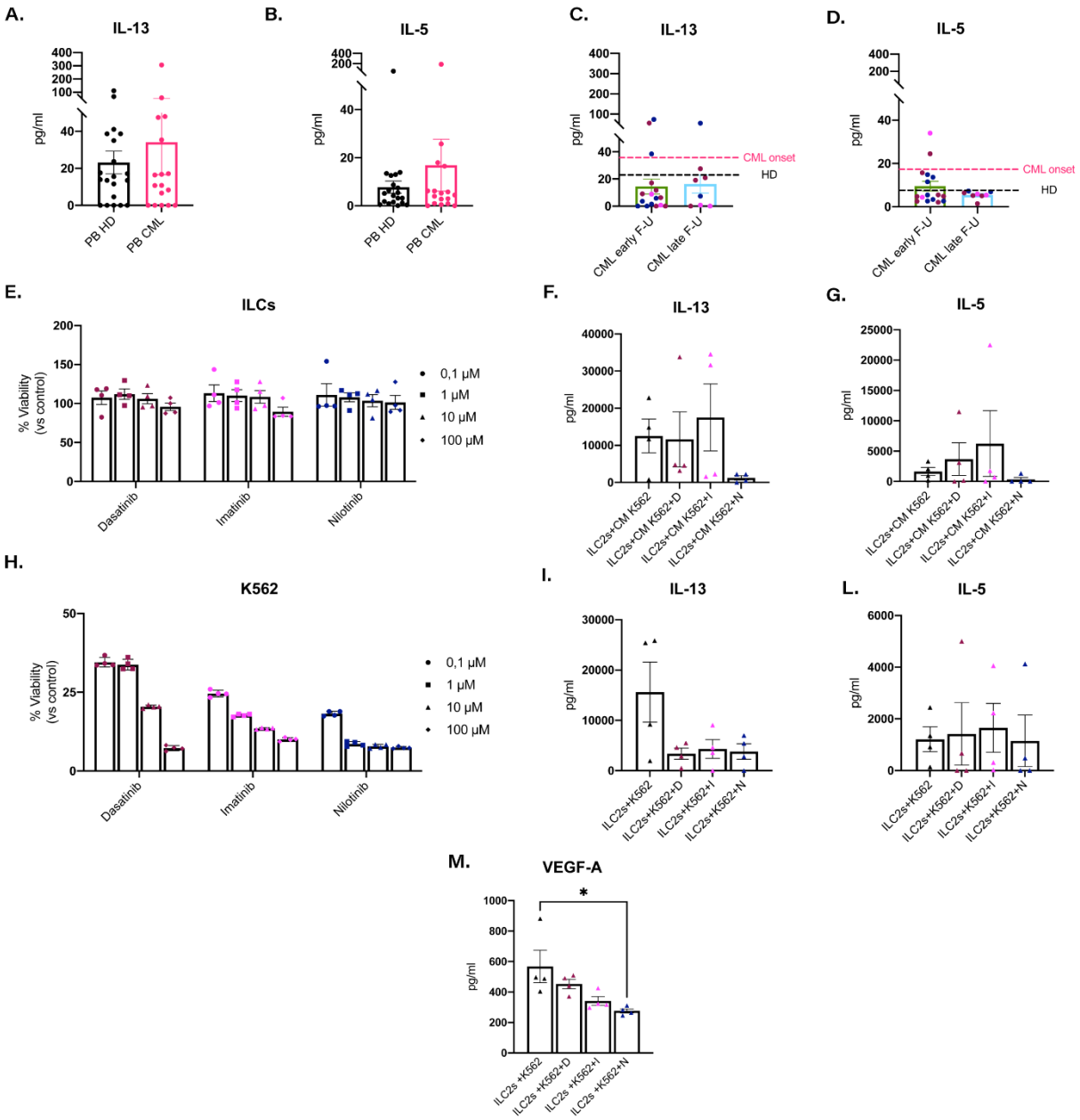

Figure S5. TKIs mainly act on tumor cells. (A-B) IL-13 and IL-5 concentrations (pg/ml) in CML patients' sera at diagnosis (n=17) versus HD (n=20). **(C-D)** IL-13 and IL-5 levels in CML sera after different treatments at early (<12 months) (n=16) or late (>12 months) (n=8) follow-ups (F-U). **(E)** MTT assay on total ILCs treated with Dasatinib, Imatinib and Nilotinib at different concentration (n=4). **(F-G)** IL-13 and IL-5 secretion (pg/ml) by ILC2s in co-culture with K562 Conditioned Medium (CM) with or without TKIs at 10µM for 48h (n=4). **(H)** MTT

assay on K562 cell line treated with Dasatinib, Imatinib and Nilotinib at different concentration (n=4). **(I-L)** IL-13 and IL-5 secretion (pg/ml) by ILC2s in co-culture with K562 cells with or without TKIs at 10μM for 48h (n=4). **(M)** VEGF-A secretion (pg/ml) in the ILC2-K562 co-culture after 48h treatment with Dasatinib, Imatinib and Nilotinib at 10μM (n=4). Statistical analysis: ordinary one-way ANOVA, *p=<0.05; **p=<0.01; ***p=<0.001; ****p=<0.0001.

Figure S6

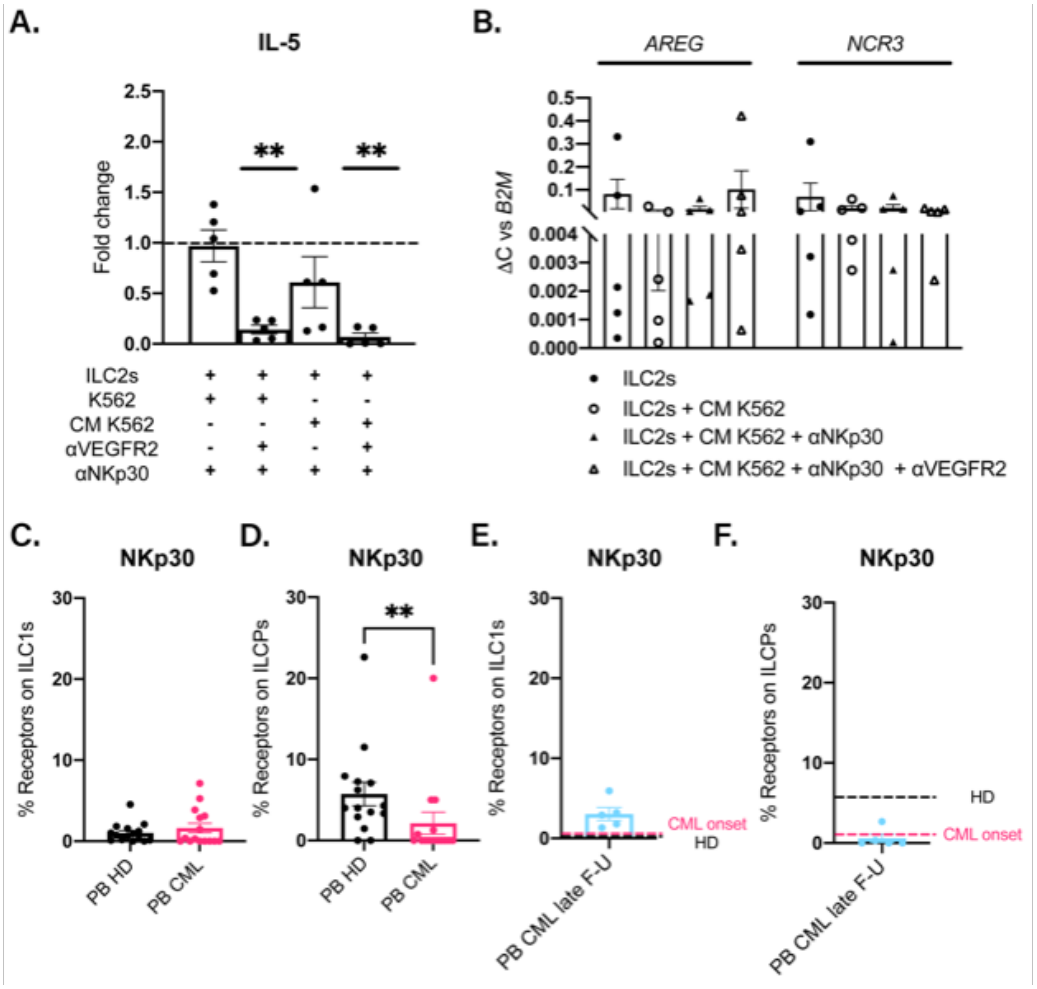

Figure S6. NKp30-B7H6 axis is not involved in ILC2-K562 crosstalk in CML. (A) Fold change of IL-5 expression after NKp30 inhibition alone or in combination with a VEGFR2 inhibitor (10μM, SU-1498) in ILC2-K562 co-cultures. Statistics were calculated compared to fold change=1 (n=5). **(B)** AREG and NKp30 (NCR3) gene expression in ILC2s stimulated with the CM of K562 in the presence or not of anti-NKp30 treatment and/or the VEGFR2 inhibitor (n=5). **(C-D)** Expression of NKp30 on ILC1s and ILCPs on HD and CML patients' PB (n=15). **(E-F)** NKp30 expression on ILC1s and ILCPs in CML patients' PB at late (>12 months) (n=5) follow-ups (F-U). Statistical analysis: Mann-Whitney test, *p=<0.05; **p=<0.01; ***p=<0.001; ****p=<0.0001.